Available online at www.sciencedirect.com
SCIENCE DIRECT
International Journal of Mass Spectrometry 249–250 (2006) 379–384
International Journal of Mass Spectrometry
www.elsevier.com/locate/ijms

Collisional stabilization of highly vibrationally excited *o*-, *m*- and *p*-xylene ions ($C_8H_{10}^+$) from 300–900 K and 1–250 Torr

Abel I. Fernandez [a,1], I. Dotan [b], Thomas M. Miller [c], J. Troe [d], Jeffrey F. Friedman [e,f], A. Viggiano [a,*]

[a] *Air Force Research Laboratory, Space Vehicles Directorate, 29 Randolph Rd., Hanscom AFB, MA 01731-3010, USA*
[b] *Department of Natural Science, The Open University of Israel, 108 Ravutski St., Raanana 43107, Israel*
[c] *Institute for Scientific Research, Boston College, USA*
[d] *Institute for Physical Chemistry, University of Göttingen, Tammannstrasse 6, D-37077 Göttingen, Germany*
[e] *Department of Physics, University of Puerto Rico, Mayaguez, 00681-9016 Puerto Rico*
[f] *Air Force Research Laboratory, Directed Energy Directorate, Kirtland Air Force Base, Albuquerque, New Mexico 87117-5776, USA*

Received 1 November 2005; received in revised form 28 November 2005; accepted 29 November 2005
Available online 18 January 2006

Abstract

Branching ratios for the reactions of O_2^+ with all three xylene isomers have been measured as a function of temperature over a wide range (300–900 K) at a fixed number density (1.45×10^{16} molecule cm^{-3} of helium) and for *m*-xylene over an extended buffer gas pressure (50–250 Torr of nitrogen) and temperature (473–623 K) range. Rate constants measured under selected conditions indicate that the reactions proceed at the collisional rate. Two main products were observed in each reaction: the stabilized parent ion, $C_8H_{10}^+$ (S) and a dissociative charge transfer product, $C_7H_7^+$ (D). The ratio of S/D was found to vary significantly with both temperature and pressure. At high pressure very little dissociation occurred. Results of statistical modeling similar to that used in our studies of *n*-alkylbenzenes represent the data well.

Keywords: Xylene; Collisional stabilization; Unimolecular dissociation; Pressure dependence; Temperature dependence

1. Introduction

There has been much interest in the study of the detection, reactivity, decomposition pathways and toxicity of xylenes because these species, as well as other aromatics and volatile organic compounds (VOCs), are involved in the use, production, destruction, combustion and accidental emissions concerning plastics, fibers, resins, power sources and fuels [1–10]. Much effort has been expended in the modeling of the effects of xylene and other VOCs on the atmosphere [11,12], and there are concerns regarding the enhancement of formation of tropospheric ozone and other health risks [13–15]. There are concomitant efforts to remove xylenes by microbial degradation, discharges and plasmas, and by ultraviolet photooxidation [2,16–19]. Moreover, the xylene isomers can be distinguished from each other by negative ion mass spectroscopy and by comparing translational energy releases [20–22].

There has also been much interest in the study of ionic xylenes. For example, there is evidence that combustion can be enhanced by ion–molecule chemistry [23]. The reactivity of various neutral and ionic aromatics, including xylenes, has been studied [24–36], in part to elucidate pathways to end products [37–41].

Recently, we have studied the kinetics of charge transfer reactions for a homologous series of *n*-alkylbenzenes (ethylbenzene, propylbenzene and butylbenzene) over wide temperature and pressure ranges [24–27,30]. We produce the highly vibrationally excited alkylbenzene by charge transfer with O_2^+. The excited species can either decompose by unimolecular dissociation or undergo collisional stabilization in collisions with a buffer gas. At higher temperatures thermal decomposition of the alkylbenzene cation also becomes important.

Malow et al. [42] recently studied the unimolecular dissociation of the xylene and ethylbenzene isomers of $C_8H_{10}^+$. They found vastly different values of $k(E)$ for the two isomers. Also,

* Corresponding author. Tel.: +1 781 377 4028; fax: +1 781 377 1148.
E-mail address: albert.viggiano@hanscom.af.mil (A. Viggiano).
[1] Postdoctoral Fellow "National Academy of Sciences", USA.

1387-3806/$ – see front matter © 2005 Elsevier B.V. All rights reserved.
doi:10.1016/j.ijms.2005.11.020

we have previously presented measurements of the ratio of stabilized parent, $C_8H_{10}^+$ (S), to the dissociation product, $C_7H_7^+$ (D), for the ethylbenzene isomer as a function of temperature and buffer gas density [26]. Detailed statistical modeling of those experiments [24] was used to determine energy transfer parameters and the details of the charge transfer mechanism. Here, we extend our studies to the measurement of *m*-, *o*- and *p*-xylene cations. Branching fractions have been measured for the *m*-xylene isomer as a function of temperature and buffer gas pressure using our turbulent ion flow tube (TIFT, high pressures and moderately high temperatures) and for all three isomers in our high temperature flowing afterglow (HTFA).

In the same fashion as our earlier work, the kinetics can be represented by the following reactions:

$$O_2^+ + C_8H_{10} \rightarrow O_2 + C_8H_{10}^+ \quad (1)$$

$$O_2^+ + C_8H_{10} \rightarrow O_2 + C_8H_{10}^{+*} \quad (2)$$

$$C_8H_{10}^{+*} \rightarrow C_7H_7^+(Bz^+, Tr^+) + CH_3 \quad (3)$$

$$C_8H_{10}^{+*} + M \rightarrow C_8H_{10}^+ + M \quad (4)$$

$$C_8H_{10}^+ (+M) \rightarrow C_7H_7^+ + CH_3 (+M) \quad (5)$$

The asterisk indicates vibrational excitation of the nascent charge transfer product; not all of these initial products have sufficient energy to dissociate. The fraction with enough energy to dissociate has been shown to be highly dependent on the charge transfer mechanism [24]. The symbols Bz^+, Tr^+ refer to the aromatic benzylium and the seven-membered tropylium ring, two isomeric forms of $C_7H_7^+$. We monitored S/D, which is the ratio of collisional stabilization to dissociation events. Our experience is that over moderate density ranges, S/D is linear, but that over extended density ranges, non-linearities occur due to the multi-state nature of the problem [24,25].

2. Experimental technique

Two apparatuses were used for these experiments. The branching ratio measurements over an extended temperature range at a fixed gas number density were made using our high-temperature flowing afterglow (HTFA) apparatus [37,43,44]. High pressure experiments were conducted only for *m*-xylene in the turbulent ion flow tube (TIFT) [26,45]. A brief description is given below for both techniques. Both of the experiments were carried out at the Air Force Research Laboratory (AFRL).

In the HTFA, a fast helium flow transported the ions, created by electron impact, through a heated quartz flow tube. A commercial furnace was used for the heating. After the gases reach equilibrium temperature, the reactant gas (*m*-, *o*- or *p*-xylene, C_8H_{10}) was added. Temperature can be varied from ambient up to 1500 K and typical pressures vary from 0.5 to 2 Torr. Here, we made measurements from 300 to 900 K at a buffer density of 1.45×10^{16} molecule cm^{-3}, with the maximum temperature limited by potential decomposition of the xylenes. The bulk of the gas was pumped by a roots blower and a small fraction was sampled before the ions were filtered by a quadrupole mass spectrometer and detected by an electron multiplier. The O_2^+ ions were made from O_2 in an electron impact ion source.

The TIFT is similar to low pressure flow tubes except that larger flow rates are used to achieve higher pressures and Reynolds numbers. Buffer gas pressure can be varied from 30 to 300 Torr and the temperature can be elevated up to 700 K. A liquid nitrogen storage vessel supplied the N_2 carrier gas, which was preheated in a sidearm. The precursor ions, O_2^+, were created upstream in an off-axis corona discharge source and were entrained into the N_2 flow in the sidearm. The feed gas to the corona consisted of a mixture of ~1% oxygen in argon. A mixture of N_2 and vapor of the neutral reagent, *m*-xylene, was injected through a moveable, axial tube into the reaction zone. Efficient charge transfer followed, producing the xylene cation, $C_8H_{10}^+$. At the end of the flow tube, most of the gas was removed by a large mechanical pump, while a small fraction was sampled through a 150 μm orifice in a truncated nosecone. The core of the ensuing supersonic expansion was sampled through a skimmer into a mass spectrometer. The ions were analyzed by a quadrupole mass filter and counted by a discrete-dynode electron multiplier.

In order to elevate the temperature, five zones of heating were used and the gas temperature was maintained to ±2 K. The main flow tube was heated in three zones, one short zone at the upstream end, a long middle section and a zone inside the vacuum chamber just upstream of the nosecone. The connection between the corona discharge tube and its sidearm was also heated. Lastly, it was found that preheating of the buffer gas was needed since the residence time was too small to cope with the decrease in heat transfer at high pressures. The preheater consisted of two Mellen split type (clam shell) tubular heating elements that surround a tubular piece of copper. The N_2 gas flowed through narrow channels (which traverse the copper tube along the axis) that have a radial-spoke cross-section. The pattern was chosen to promote efficient heating.

In both apparatuses, the O_2^+ primary ion comprised >98% of the primary ions. When a neutral xylene reactant was added, product ions at 91 amu ($C_7H_7^+$), 106 amu ($C_8H_{10}^+$) and 119 amu ($C_9H_{11}^+$) were observed in the mass spectra of the TIFT and HTFA experiments. The first of these ions is a fragment that can exist as the aromatic benzylium isomer or as the seven-membered tropylium isomer. The second is the non-dissociative charge transfer product ion, which will be different dependent on the isomer of xylene studied. The third ion is due to secondary chemistry of the benzylium cation with neutral reactant [46]. Effects of secondary chemistry were eliminated by varying the xylene reactant concentration and extrapolating to zero. Operating the TIFT at 698 K and 80 Torr, a high resolution spectrum of the *m*-xylene reaction showed a small amount of mass 105, indicating the loss of a hydrogen atom. This product has been observed when the xylene cation has high internal energy, in the Malow et al. experiments [42]. The only appreciable dissociative charge transfer product was $C_7H_7^+$, at 91 amu. The species $C_7H_8^+$ was not observed with xylene, unlike our earlier studies of *n*-propylbenzene [25] and *n*-butylbenzene [27], because the alkyl sidechain of the xylenes are not long enough to promote the McLafferty rearrangement needed for this fragmentation chan-

nel. The mass spectra exhibited common impurities due to a water impurity in the buffer; $H_3O^+(H_2O)_{0,1}$ and $O_2^+(H_2O)$. The impurities were less than 2% (sometimes much less) in both apparatuses. No corrections to the recorded branching ratios were made since the impurities were small and it was not clear how to make corrections accurately. However, since the dissociative product was small, a part of the scatter in the data may result from the impurities.

The following source gases were used for the experiments. He (AGA, 99.995%) was used as the buffer gas in the HTFA after passing through a liquid nitrogen trap to remove water vapor. Boil off from liquid nitrogen was used as the buffer in the TIFT. O_2 (Mass. oxygen, 99.999%) was used as the source gas to produce O_2^+ in both experiments. Approximately, 1% mixtures of *o*-xylene (Aldrich, 97%, anhydrous), *p*-xylene (Aldrich, 99+%, HPLC grade) and *m*-xylene (Aldrich, 99+%, anhydrous) in helium were used as the reactant neutrals. The vapors from the xylenes were used after several freeze–thaw cycles.

3. Results

In the present work, the main goal was to measure branching ratios as a function of temperature and pressure. This requires a low depletion of $[O_2^+]$ which is necessary to account for the secondary chemistry but adds uncertainty to measurements of rate constants. In addition, rate constants in the HTFA have been found to be sensitive to experimental condition, but branching ratios have not. Since, we were fixing the buffer gas number density in those experiments, it was not possible to optimize for accurate rate constant measurements. In addition, previous studies of the reactions of O_2^+ with alkylbenzenes showed that reaction occurred on every collision for all conditions [25,26,47]. The extra effort required to measure rate constants at each set of conditions is time consuming using the current experimental arrangement. Therefore, we only spent time testing the assumption of a collisional rate constant for the *m*-xylene system in the TIFT at pressures less than 100 Torr. Above this pressure, substantially more observation time was necessary for experimental reasons. The average of the measurements of rate constants below 100 Torr was 2.1×10^{-9} cm^3 molecule^{-1} s^{-1} over the temperature range of 473–623 K. This value is in good agreement with our previous room temperature measurement (1.7×10^{-9} cm^3 molecule^{-1} s^{-1}) and with those of Španěl and Smith (1.9×10^{-9} cm^3 molecule^{-1} s^{-1}). Both of these measurements were performed using the selected-ion flow tube (SIFT) technique [23,28,29].

The remainder of the experimental results consists of measurements of the branching ratio $[C_8H_{10}^+]/[C_7H_7^+]$, or S/D, as a function of temperature and pressure. The HTFA was used to measure the temperature dependence of S/D at a fixed bath gas concentration for all three xylene ion isomers, from 300 to 900 K. The results are shown in Fig. 1. The buffer gas number density was kept at a constant value (1.45×10^{16} molecule cm^{-3}) in order to separate temperature effects from those of collisions. The Langevin collision rate constant of the excited xylene ion with He buffer is 5.5×10^{-10} cm^3 molecule^{-1} s^{-1}, independent of temperature. Therefore, fixing the buffer gas number density

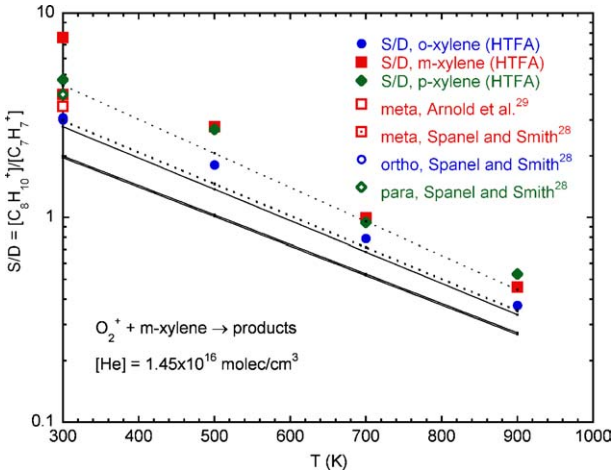

Fig. 1. HTFA measurements for S/D of *m*-, *o*- and *p*-xylene cations from 300 to 900 K at a constant number density of the bath gas He of 1.45×10^{16} molecule cm^{-3}. The present data at each temperature are an average of three to six individual points. Also shown are room temperature results from Ref. [29] (□) and from Ref. [28] (□, ◯ and ◊). The full lines (in order of *p*-, *o*- and *m*-xylene from top to bottom) present the results of a modeling with $-\langle\Delta E\rangle/hc = 180$ cm^{-1}, the dashed lines with 360 cm^{-1}, see text.

fixes the time between collisions. Similarly, the Langevin collision rate with the N_2 buffer used in the TIFT is independent of temperature at 6.6×10^{-10} cm^3 molecule^{-1} s^{-1}.

Fig. 1 shows not only the present HTFA data but also room temperature values of S/D taken at similar number densities from other experiments. The agreement for *o*-xylene and *p*-xylene is good to excellent. In contrast, that for *m*-xylene is less satisfactory. The present value for S/D of about 7.6 compares to previous SIFT values of 3.5 and 4 [28,29]. No good explanation is apparent for the discrepancy, especially given the good agreement for the other two isomers. The measurements were repeated a number of times as a check, and S/D remained higher than values reported in earlier work.

If the present value of S/D for *m*-xylene at 300 K is rejected, then the S/D values follow the inequality: para ∼ meta > ortho. Two sets of model lines are shown in Fig. 1, which rationalizes the absolute values and temperature dependences of the results. The relative values of the para and ortho isomers are well predicted. The model predicts relative values for the meta isomer to be more like the para isomer. However, agreement with either the para or ortho results is within the uncertainties of the model given that only very small differences in energetics are needed to explain the differences. The details of the modeling are given below.

The pressure dependence of collisional stabilization was measured using the TIFT over a buffer gas pressure range of 50–250 Torr and temperatures from 473 to 623 K for the *m*-xylene only. These data are shown in Fig. 2. Measurements of S/D were made also at 698 K, but these higher temperature results exhibited very large scatter and were thus discarded. The TIFT has not yet been well characterized at such high temperatures. The values of S/D are very large indicating that little dissociation occurs at these high pressures.

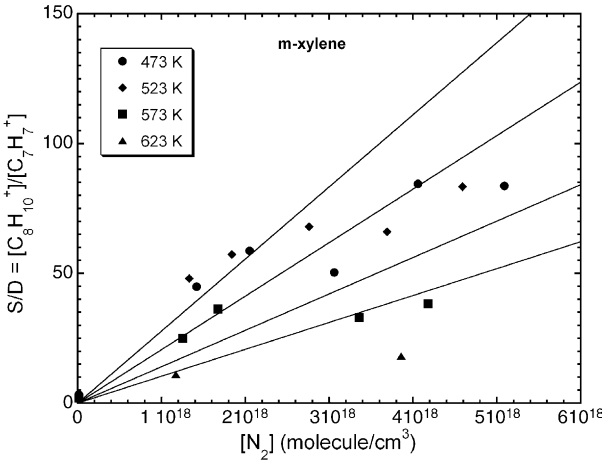

Fig. 2. TIFT measurements of S/D for the *m*-xylene cation as a function of number density of N_2 (50–250 Torr) over the temperature range 473–623 K. Te lines for $T = 473$, 523, 573 and 623 K (from top to bottom) show modeling results with $-\langle\Delta E\rangle/hc = 280\ \mathrm{cm}^{-1}$, see text.

Compared to our earlier experiments for ethylbenzene [26], *n*-propylbenzene [25] and *n*-butylbenzene [27] much larger values of S/D were observed for xylene. Our modeling given below indicated that, for these large values of S/D, there should be a nearly linear dependence of S/D on $[N_2]$ with $S/D \approx 0$ at $[N_2] = 0$. The modeled curves are also shown in Fig. 2. One observes some scatter around these curves. However, the trends are quite clear: at a given T, S/D increases with $[N_2]$ because of more efficient collisional stabilization and, at a given $[N_2]$, S/D decreases with increasing T because of increasing energy and hence an increasing dissociation rate.

The kinetics outlined in Section 1 can be analyzed for S/D. In its simplest form (assuming a single excited state) this can be written as:

$$\frac{S}{D} = \frac{[C_8H_{10}^+]}{[C_7H_7^+]} \approx \frac{\alpha}{1-\alpha} + \frac{\gamma_c Z[N_2]}{(1-\alpha)k(E)} \tag{6}$$

where E denotes the internal energy of the chemically activated xylene cations, γ_c the collision efficiency (for stabilization) and $k(E)$ is the specific rate constant for their fragmentation. We identify Z with the collision rate constant, being the Langevin capture rate constant between $C_8H_{10}{}^+$ and M. Finally, the symbol α corresponds to the fraction of nascent xylene cations that do not have enough energy to decompose, $k_1/(k_1 + k_2)$. This expression predicts a linear dependence of S/D with pressure or number density. A more detailed modeling identifying $(1-\alpha)$ in terms of the branching of the charge transfer channels is given below.

4. Modeling

In the following, we demonstrate that our measured S/D as a function of temperature T and bath gas concentration [M] can well be accounted for by the modeling scheme elaborated in our work on other alkylbenzenes [24,25,27,47,48]. However, lack of information on a few of the input data required for the modeling leaves some arbitrariness in the finer details.

Our earlier studies of the reaction of $O_2{}^+$ with alkylbenzenes clearly showed that the charge transfer processes (1) and (2) can proceed by three mechanisms: resonant charge transfer (branching ratio g_a) which essentially deposits the thermal energy of the neutral alkylbenzene (C_8H_{10} in this paper) into the parent ion ($C_8H_{10}{}^{+*}$) in addition to the difference of the ionization energies of O_2 and the alkylbenzene, complex-forming charge transfer (branching ratio g_b) which statistically distributes the energy, and charge transfer producing electronically excited O_2 (branching ratio g_c). Modeling the corresponding energy distributions $g(E, T)$ has been done in our work analogous to that described previously [24,25,27]. We use g_a and g_b as parameters, while $g_c = 1 - g_a - g_b$. The second set of input parameters needed to model the data are the average energies $\langle\Delta E\rangle$ transferred per collision between vibrationally highly excited $C_8H_{10}{}^{+*}$ and the buffer gas M. We use $\langle\Delta E\rangle$ values such as obtained from our analysis of the collisional stabilization of ethylbenzene cations [24]. Finally, we require information on the specific rate constants $k(E)$ for dissociation of $C_8H_{10}{}^{+*}$. For the latter quantity, in our energy range we only have relatively uncertain single-energy measurements from photodissociation experiments [35]. There are low energy measurements for *o*-xylene [42], which, however, seem to have a very unusual energy dependence and do not seem compatible with the single higher energy point. In this situation, we must live with uncertainty of the input parameters and to accept some deviation between the modeling and the experimental results.

We use collisional stabilization rate constants $\gamma_c Z[M]$ with the collision efficiency γ_c approximated by [49]:

$$\frac{\gamma_c}{1-\gamma_c^2} \approx \frac{-\langle\Delta E\rangle s^*}{E - E_0} \tag{7}$$

where E_0 denotes the dissociation threshold energy for reaction (3) and the specific rate constants $k(E)$ of reaction (3) are represented approximately by:

$$k(E) \propto (E - E_0)^{s^*-1} \tag{8}$$

S/D then is derived from:

$$\frac{S}{D} = Z[M] \int_0^\infty dE\, g(E, T) \frac{\gamma_c(E)}{k(E)} \tag{9}$$

where S^* is a fit variable.

As done previously for ethylbenzene cations, [24] we combine the single energy measurement [35] for *o*-xylene of $k(E) = 7\ (\pm 3) \times 10^8\ \mathrm{s}^{-1}$ at an energy of $E/hc \approx 35{,}090\ \mathrm{cm}^{-1}$, with $k(E) = 3 \times 10^4\ \mathrm{s}^{-1}$ at $E/hc = 23{,}170\ \mathrm{cm}^{-1}$ in the middle of the experiments from Ref. [42]. This leads to

$$k(E) \approx 7(\pm 3) \times 10^8 \left[\frac{E - E_0}{hc\ 35{,}090\ \mathrm{cm}^{-1}}\right]^{5.85} \tag{10}$$

with $E_0/hc = 16{,}890\ \mathrm{cm}^{-1}$. The exponent is similar to the value of 4.824 derived for ethylbenzene cations [27], but differs markedly from a value of 17.93 derived in Ref. [42]. As our measurements are made at energies close to the single high energy datum, the representation of Eq. (10) appears to be much more meaningful than that given for the low energy data alone.

Table 1
Molecular parameters employed in the modeling

Molecule	Ionization energy (eV)[a]	Dissociation energy at 0 K (kJ mol^{-1})[b]	Vibrational frequencies
o-Xylene	8.56	202	Ref. [51]
m-Xylene	8.55	205	Ref. [51]
p-Xylene	8.44	215	Ref. [42]

[a] Ref. [50].
[b] Ref. [50], with conversion from 298 to 0 K as in Ref. [35].

Keeping the same exponent as for *o*-xylene, the single-energy measurements [35] for the other xylenes correspond to

$$k(E) \approx 5(\pm 3) \times 10^8 \left[\frac{(E - E_0)}{hc\, 36,050\,\mathrm{cm}^{-1}}\right]^{5.85} \quad (11)$$

with $E_0/hc = 17{,}970\,\mathrm{cm}^{-1}$ for *p*-xylene and

$$k(E) \approx 8(\pm 3) \times 10^8 \left[\frac{(E - E_0)}{hc\, 35,170\,\mathrm{cm}^{-1}}\right]^{5.85} \quad (12)$$

with $E_0/hc = 17{,}140\,\mathrm{cm}^{-1}$ for *m*-xylene; see Table 1 for the molecular data employed. $|\langle\Delta E\rangle|$-values for M = He of 180 ($\pm$90) cm^{-1} and for M = N_2 of 285 ($\pm$150) cm^{-1} were taken from Ref. [24]. Likewise, initial branching ratios were taken from Ref. [24]. However, we found that $g_c = 0.1$, rather than $g_c = 0.183$ used in Ref. [24], gives slightly better agreement with the experimental slopes of the lines shown in Fig. 1. Therefore, we use $g_a = 0.45$, $g_b = 0.45$ and $g_c = 0.1$ to initialize the modeling.

The effective γ_c-values are much smaller than unity such that γ_c is essentially proportional to $\langle\Delta E\rangle$. Therefore for large values of S/D such as displayed in Fig. 2, the slope of S/D-plots is sensitive to the ratio of $\langle\Delta E\rangle/k(E)$ where the effective energy depends on g_a and g_b. On the other hand, the small values of S/D such as shown in Fig. 1 are also sensitive, at fixed g_a, to the partitioning of $1 - g_a$ between g_b and g_c. This applies in particular to the slope of the temperature dependences in Fig. 1. In contrast, the TIFT measurements shown in Fig. 2 are relatively insensitive to the value of g_c. We, therefore, first optimized g_c by inspecting Fig. 1. We found that there was a small dependence on g_c with $g_c = 0.1$ reproducing best the experimental temperature dependences. In order to reproduce the absolute values of S/D, we had to take into consideration the considerable uncertainty of the ratio $\langle\Delta E\rangle/k(E)$ discussed above. The full lines in Fig. 1 used $-\langle\Delta E\rangle/hc = 180\,\mathrm{cm}^{-1}$ for M = He, such as determined for ethylbenzene cations in Ref. [24]. Increasing $|\langle\Delta E\rangle|$ by a factor of 2 yields the dashed lines shown in Fig. 1. These are in better agreement with the experiments. However, the uncertainty in $k(E)$ as well as in the energy distributions after charge transfer amounts to a factor of two uncertainty. For this reason, we cannot draw conclusions about the value of $\langle\Delta E\rangle$ better than a factor of two. A similar uncertainty was encountered in Ref. [24].

Our modeling of the high pressure values of S/D for *m*-xylene shown in Fig. 2 led to the lines given in the figure. In this case, the use of $k(E)$ from Eq. (12), $-\langle\Delta E\rangle/hc = 285\,\mathrm{cm}^{-1}$ such as derived for ethylbenzene cations[26] with M = N_2, and $g_a = 0.45$ like for ethylbenzene (together with $g_b = 0.45$ and $g_c = 0.1$), directly gave agreement within our experimental scatter such that fine-tuning of the modeling results did not appear meaningful. One should note that thermal dissociation did not play any role for the conditions of the experimental results shown in Fig. 2.

5. Conclusions

The combination of our experimental and modeling results show an internally consistent picture. The reaction of O_2^+ with the three xylene isomers presents itself as a chemical activation system where the initial charge transfer proceeds by three channels, i.e., by resonant, complex-forming and electronic excitation charge transfer pathways. This is similar to the modeling for the corresponding ethyl-, *n*-propyl- and *n*-butylbenzene systems. Having accounted for the superposition of the energy distributions from these three channels, dissociation of xylene cations competing with collisional stabilization needed to be analyzed by a master equation. In our treatment this was done in a simplified manner with the equations derived from a step-ladder model. Employing specific rate constants from the literature as well as charge transfer branching ratios and collisional energy transfer properties such as derived for ethylbenzene cations, the measured stabilization versus dissociation yields could be reproduced within a factor of two in detail without further parameter adjustments. One can, therefore, conclude that the observed properties of the considered reactions can be well rationalized by our approach.

Acknowledgements

It is a pleasure to have this paper in a memorial issue to Chava Lifshitz. She had been a leading ion chemist and made excellent contributions to the understanding of the decomposition of alkylbenzenes, the subject of this paper. One of us (I.D.) had collaborated with Chava for many years and appreciates all she taught him. We dedicate this paper to her memory as a great scientist, teacher and friend.

This work has been supported by funding through the Deutsche Forschungsgemeinschaft (SFB 357 “Molekulare Mechanismen unimolekularer Prozesse”), the European Office for Aerospace Research (EOARD Grant No. FA 8655-03-1-3034) and the United States Air Force Office of Scientific Research (Project 2303 EP4). T.M.M. is under contract (FA8718-04-C0006) to the Institute for Scientific Research of Boston College.

References

[1] A.G. Kraabøl, P. Konopka, F. Stordal, H. Schlager, Atmos. Environ. 34 (2000) 3939.
[2] M. Mohseni, L.-H. Koh, D.C.S. Kuhn, D.G. Allen, J. Environ. Eng. Sci. 4 (2005) 279.
[3] E. Zervas, X. Montague, J. Lahaye, Fuel 83 (2004) 2313.
[4] A. Roubaud, R. Minetti, L.R. Sochet, Combust. Flame 121 (2000) 535.
[5] A. Roubaud, O. Lemaire, R. Minetti, L.R. Sochet, Combust. Flame 123 (2000) 561.
[6] P. Mattrel, A.-M. Vasic, E. Gujer, R. Haag, M. Weilenmann, Int. J. Environ. Pollut. 22 (2004) 301.

[7] J.I. Baumbach, S. Sielemann, Z. Xie, H. Schmidt, Anal. Chem. 75 (2003) 1483.
[8] H. Borsdorf, H. Schelhorn, J. Flachowsky, H.-R. Döring, J. Stach, Anal. Chim. Acta 403 (2000) 235.
[9] S. Wolfe, Z. Shi, Can. J. Chem. 79 (2001) 1278.
[10] X.M. Feng, X.P. Ai, H.X. Yang, J. Appl. Electrochem. 34 (2004) 1199.
[11] J.R. Odum, T.P.W. Jungkamp, R.J. Griffin, R.C. Flagan, J.H. Seinfeld, Science 276 (1997) 96.
[12] M.E. Jenkin, S.M. Saunders, V. Wagner, M.J. Pilling, Atmos. Chem. Phys. 3 (2003) 181.
[13] M.E. Jenkin, K.C. Clemitshaw, Atmos. Environ. 34 (2000) 2499.
[14] M.-L. Chen, S.-H. Chen, B.-R. Guo, I.-F. Mao, J. Environ. Monit. 4 (2002) 562.
[15] A.M. Saillenfait, F. Gallissot, G. Morel, P. Bonnet, Food Chem. Toxicol. 41 (2003) 415.
[16] P.J.S. Colberg, L.Y. Young, in: L.Y.Y.A.C.E. Cerniglia (Ed.), Microbial Transformation and Degradation of Toxic Organic Chemicals, Wiley, New York, 1995, p. 307.
[17] H.-H. Kim, A. Ogata, S. Futamura, J. Phys. D: Appl. Phys. 38 (2005) 1292.
[18] H.M. Lee, M.B. Chang, Plasma Chem. Plasma Process. 23 (2003) 541.
[19] D.T. Gibson, V. Mahadevan, J.F. Davey, J. Bacteriol. 119 (1974) 930.
[20] J.M. Curtis, R.K. Boyd, B. Shushan, T.G. Morgan, J.H. Beynon, Org. Mass Spectrom. 19 (1984) 207.
[21] E.S. Mukhtar, I.W. Griffiths, F.M. Harris, J.H. Beynon, Org. Mass Spectrom. 16 (1981) 51.
[22] A.G. Harrison, H.Y. Tong, Org. Mass Spectrom. 23 (1988) 135.
[23] S. Williams, A.J. Midey, S.T. Arnold, T.M. Miller, P.M. Bench, R.A. Dressler, Y.-H. Chiu, D.J. Levandier, A.A. Viggiano, R.A. Morris, M.R. Berman, L.Q. Maurice, C.D. Carter, AIAA 2001-2873 4th Weakly Ionized Gases Workshop, 2001.
[24] J. Troe, A.A. Viggiano, S. Williams, J. Phys. Chem. A 108 (2004) 1574.
[25] A.I. Fernandez, A.A. Viggiano, T.M. Miller, S. Williams, I. Dotan, J.V. Seeley, J. Troe, J. Phys. Chem. A 108 (2004) 9652.
[26] A.A. Viggiano, T.M. Miller, S. Williams, S.T. Arnold, J.V. Seeley, J.F. Friedman, J. Phys. Chem. A 106 (2002) 11917.
[27] A.I. Fernandez, A.A. Viggiano, J. Troe, J. Phys. Chem. A, submitted for publication.
[28] P. Spanel, D. Smith, Int. J. Mass Spectrom. Ion Process. 181 (1998) 1.
[29] S.T. Arnold, I. Dotan, S. Williams, A.A. Viggiano, R.A. Morris, J. Phys. Chem. A 104 (2000) 928.
[30] S. Williams, A.J. Midey, S.T. Arnold, R.A. Morris, A.A. Viggiano, Y.-H. Chiu, D.J. Levandier, R.A. Dressler, M.R. Berman, J. Phys. Chem. A 104 (2000) 10336.
[31] A.W. Castleman Jr., Annu. Rev. Phys. Chem. 45 (1994) 685.
[32] D.I. Rosen, G. Weyl, J. Phys. D: Appl. Phys. 20 (1987) 1264.
[33] J. Grotemeyer, H.-F. Grützmacher, Org. Mass Spectrom. 17 (1982) 353.
[34] J. Grotemeyer, H.-F. Grützmacher, in: M.L. McGlashan (Ed.), Current Topics in Mass Spectrometry and Chemical Kinetics: Proceedings of the Symposium in Honour of Professor Allan Maccoll on the Occasion of his Retirement from University College, London, Heyden, London, 1982, p. 29.
[35] Y.H. Kim, J.C. Choe, M.S. Kim, J. Phys. Chem. A 105 (2001) 5751.
[36] D. Kuck, Mass Spectrom. Rev. 9 (1990) 187.
[37] A.J. Midey, S. Williams, S.T. Arnold, I. Dotan, R.A. Morris, A.A. Viggiano, Int. J. Mass Spectrom. 195/196 (2000) 327.
[38] E.S.C. Kwok, S.M. Aschmann, R. Atkinson, J. Arey, J. Chem. Soc. Faraday Trans. 93 (1997) 2847.
[39] C. Rebrion-Rowe, T. Mostefaoui, S. Laubé, J.B.A. Mitchell, J. Chem. Phys. 113 (2000) 3039.
[40] M.A. Mawid, T.W. Park, B. Sekar, C. Arana, AIAA 2003-4938 39th AIAA/ASME/SAE/ASEE Joint Propulsion Conference and Exhibit, 2003.
[41] M.A. Mawid, T.W. Park, B. Sekar, C. Arana, AIAA 2004-4207 40th AIAA/ASME/SAE/ASEE Joint Propulsion Conference and Exhibit, 2004.
[42] M. Malow, M. Penno, K.-M. Weitzel, J. Phys. Chem. 107 (2003) 10625.
[43] P.M. Hierl, J.F. Friedman, T.M. Miller, I. Dotan, M. Mendendez-Barreto, J. Seeley, J.S. Williamson, F. Dale, P.L. Mundis, R.A. Morris, J.F. Paulson, A.A. Viggiano, Rev. Sci. Inst. 67 (1996) 2142.
[44] S.T. Arnold, S. Williams, I. Dotan, A.J. Midey, R.A. Morris, A.A. Viggiano, J. Phys. Chem. A 103 (1999) 8421.
[45] S.T. Arnold, J.V. Seeley, J.S. Williamson, P.L. Mundis, A.A. Viggiano, J. Phys. Chem. A 104 (2000) 5511.
[46] J.A. Jackson, S.G. Lias, P. Ausloos, J. Am. Chem. Soc. 99 (1977) 7515.
[47] A.A. Viggiano, A.I. Fernandez, J. Troe, Phys. Chem. Chem. Phys. 7 (2005) 1533.
[48] T.D. Fridgen, T.B. McMahon, J. Troe, A.A. Viggiano, A.J. Midey, S. Williams, J. Phys. Chem. A 108 (2004) 5600.
[49] J. Troe, J. Phys. Chem. 87 (1983) 1800.
[50] P.J. Linstrom, W.G. Mallard, NIST Chemistry WebBook, NIST Standard Reference Database No. 69, National Institutes of Standards and Technology, Gaithersburg, MD, 2003.
[51] J. Draeger, Spectrochim. Acta 41A (1985) 607.